Journal of Membrane Science 593 (2020) 117392

Contents lists available at ScienceDirect

Journal of Membrane Science

journal homepage: www.elsevier.com/locate/memsci

Improved reverse osmosis thin film composite biomimetic membranes by incorporation of polymersomes

Radosław Górecki[a,b,*], Dennis Maik Reurink[c], Muntazim Munir Khan[b], Victoria Sanahuja-Embuena[a,b], Krzysztof Trzaskuś[b], Claus Hélix-Nielsen[a]

[a] Department of Environmental Engineering, Technical University of Denmark, Bygningstorvet 115, 2800, Kongens Lyngby, Denmark
[b] Aquaporin A/S, Nymøllevej 78, 2800, Kongens Lyngby, Denmark
[c] Membrane Science & Technology, University of Twente, MESA+ Institute for Nanotechnology, P.O. Box 217, 7500, AE Enschede, the Netherlands

ARTICLE INFO

Keywords:
Aquaporin
Biomimetic membrane
Block copolymers
Polymersomes
Interfacial polymerization

ABSTRACT

Biomimetic aquaporin-based membranes offer great promise as a disruptive water treatment technology, due to their potential of improving membrane permeability without compromising solute rejection. However, fabrication upscaling is challenging and therefore the technological potential of biomimetic membranes remains unused. We propose an easily upscalable process based on bulk hydration of diblock and triblock copolymer mixture for preparation of polymersomes which can reconstitute aquaporin proteins. Such polymersomes are incorporated into biomimetic membranes via polyamide active layer synthesis based on interfacial polymerization. By incorporation of blank polymersomes, it was possible to improve water permeability of the membrane by 30%, and by incorporation of aquaporin reconstituting polymersomes by 50%, compared to the membranes without polymersomes. In both cases NaCl rejection was not affected. X-ray photoelectron spectroscopy measurements confirmed incorporation of copolymers prepared with aquaporins into the active polyamide layer without affecting the thickness of the membrane's active layer and surface zeta-potential.

1. Introduction

Ensuring access to water and sanitation for all is goal number 6 of the United Nation Sustainability Goals [1]. Not only the demand for water is increasing across all sectors [2], the problems with water quality are growing on a global scale, even in regions considered as water-rich. In both developing and industrialized nations more contaminants, including trace organics such as pharmaceuticals and pesticides to heavy metals, are entering the water due to human activities [3,4], which drives the development of more efficient water purification technologies [4,5].

As a result of a high energy efficiency and manufacturing scalability combined with a small footprint [4,6], membrane technology becomes leading technology for high quality water purification [7]. For example, polyamide based reverse osmosis (RO) membranes are used worldwide for processes such as desalination [4], water reuse [8] and domestic tap water purification [9]. These membranes are mainly thin film composite (TFC) membranes with a thin (100–200 nm) polyamide (PA) active layer (AL) coated on a porous substrate which is supported by a non-woven fabric [10]. The broad application of TFC membranes has been accompanied by continuous performance improvements resulting in enhanced water permeability, high solute rejection, low energy demand and low fouling-ability [11].

Recently, biomimetic approaches have attracted considerable interest [12]. Here, the membrane AL is doped with transmembrane proteins facilitating water transport exemplified by the use of the bacterial aquaporin protein isoform Aquaporin Z (AqpZ) [12,13]. However, industrial scale production and incorporation of aquaporins into the AL is not a trivial task due to the need for elaborate protein purification and stabilization steps [14].

A common approach for AqpZ membrane incorporation is based on reconstitution into amphiphilic liposomes or polymersomes preserving the ternary and quaternary structure of the AqpZ and thus their functionality [10,15]. Both liposomes and polymersomes have been applied in preparation for RO, forward osmosis (FO) and nanofiltration (NF) biomimetic membranes [10]. Polymersomes appear advantageous over liposomes for industrial applications due to their superior physical and chemical stability [16] as well as the possibility of introducing active groups for covalent bonding to the membrane AL [17]. However, the protein activity is generally reported to be lower in polymersomes compared to liposomes, presumably due to the increased hydrophobic mismatch between the hydrophobic polymer core layer thickness and

* Corresponding author. Department of Environmental Engineering, Technical University of Denmark, Bygningstorvet 115, 2800, Kongens Lyngby, Denmark.
E-mail addresses: rgor@env.dtu.dk, rgo@aquaporin.com (R. Górecki).

https://doi.org/10.1016/j.memsci.2019.117392
Received 13 May 2019; Received in revised form 30 July 2019; Accepted 19 August 2019
Available online 19 August 2019
0376-7388/

transmembrane protein length [18]. In order to achieve efficient functional reconstitution of AqpZ proteins into polymersomes, the polymer matrix must resemble natural phospholipid membranes while preserving the advantages in stability. For example, AqpZ can be successfully reconstituted in triblock copolymers containing polydimethylsiloxane (PDMS) [19–22]. The conformational flexibility of the PDMS blocks allows insertion of membrane proteins where the polymer chains can adapt to the fixed dimensions of the proteins [18] and protein insertion can be further increased by addition of detergents [23]. Still, reconstitution of AqpZ with triblock copolymers containing less flexible polymer chains is possible and was reported for systems such as *block*-poly(isobutylene)-*block*-poly(ethylene glycol)-*block*-poly (isobutylene) (PIB-PEG-PIB) [24] or *block*-poly(ethylene glycol)-*block*-poly(propylene glycol)-*block*-poly(ethylene glycol) (PEG-PPG-PEG) [25].

The use of AqpZ liposomes (AQP-liposomes) has been reported for the manufacturing of TFC RO membranes, TFC nanofiltration (NF) membranes, and FO membranes [26–28]. AQP-liposome TFC RO membranes showed improvements in water permeability of up to 40% when compared to commercial membranes [26] and FO membranes with AQP-liposomes, achieved a water flux of 49.1 $Lm^{-2}h^{-1}$ coupled with specific reverse salt flux of 0.10 gL^{-1} (with 1 M NaCl as draw solution and deionised (DI) water as feed) [28]. However, natural lipids are prone to oxidation which has inspired the use of amphiphilic block copolymers, as they have a higher chemical and physical stability [16,21,29]. Moreover, the use of amphiphilic block copolymers allows for the introduction of active groups to the AQP-polymersomes that can participate in interfacial polymerization (IP) and thus be covalently bonded to the PA layer [20,21,30,31].

AqpZ-embedded polymersomes (AQP-polymersomes) made by amphiphilic block copolymers have been used in TFC membranes made via IP for FO [32]. However, for the applications in which transport through the TFC membrane is driven by a hydraulic transmembrane pressure gradient, the incorporation of AQP-polymersomes has not been reported yet. Moreover, the use of membranes with AQP-polymersomes has been limited to NF membranes with limited selectivity towards monovalent ions [30,31,33,34]. Another limitation for biomimetic membranes arises from challenges in manufacturing process scalability. The preparation of AQP-polymersomes reported in the literature has been limited to film rehydration techniques [19,21,22,30,31]. The major drawback of this technique stems from the high cost due to several processing steps and product losses [35,36].

Here we propose a novel, fully scalable method to prepare and introduce AQP-polymersomes into the AL of RO membranes. First, AqpZ proteins are functionally reconstituted into AQP-polymersomes, using an industrially scalable process based on bulk hydration and self-assembly of poly-2-methyl-2-oxazoline-*block*-poly(dimethylsiloxane) (PMOXA-PDMS) and poly(2-methyl-2-oxazoline)-*block*-poly(dimethylsiloxane)-*block*-poly(2-methyl-2-oxazoline) (PMOXA-PDMS-PMOXA) copolymers with the addition of amine terminated poly(dimethylsiloxane) (A-PDMS). Secondly, AQP-polymersomes are successfully embedded into the membrane AL using the IP reaction between m-phenylenediamine (MPD) and trimesoyl chloride (TMC). This results in membranes with improved water permeability that maintain a high NaCl rejection.

2. Experimental

2.1. Preparation of polymersomes

Polymersomes were prepared by the self-assembly method in an aqueous solution of phosphate buffered saline (PBS). PBS (pH 7.2, 136 mM NaCl, 2.6 mM KCl) was prepared by dissolving 8 g NaCl, 0.2 g KCl, 1.44 g Na_2HPO_4 and 0.24 g of KH_2PO_4 in 800 mL Milli Q purified H_2O, adjusting the pH to 7.2 with HCl and bringing the volume to 1 L with Milli Q H_2O [37]. All chemicals were analytical grade (Sigma Aldrich, Denmark). Polymersomes incorporating AqpZ (AQP-1) were prepared from a mixture of AqpZ protein and diblock PMOXA-PDMS and triblock PMOXA-PDMS-PMOXA amphiphilic copolymer, according to the procedure described in the patent of Spulber and Gerstandt [37]. Briefly, 112 mg of mixture of diblock PMOXA-PDMS and triblock amphiphilic copolymer PMOXA-PDMS-PMOXA (Aquaporin A/S, Denmark) and 100 µL of aminopropyl terminated polydimethylsiloxane (A-PDMS) (Aquaporin A/S, Denmark) were mixed with 100 µL of AqpZ-stock solution (5 mg/mL) (Aquaporin A/S, Denmark) and subsequently dissolved in 100 mL PBS with 0.05% Lauryldimethylamine *N*-oxide (LDAO) (Carbosynth Ltd., United Kingdom) and 0.5% solubilizer Kolliphor® HS 15 (KHS) (Sigma-Aldrich Denmark A/S, Denmark). The resulting solution was then stirred at 170 rpm for 10 h at room temperature. Subsequently, the solution was firstly filtered through 0.45 µm polyethersulfone (PES) filter and secondly through 0.20 µm PES filter (Sarstedt, Germany). The polymersomes without AqpZ (AQP-0) were prepared in exactly the same procedure, without adding AqpZ-stock to the solution.

2.2. Characterization of polymersomes and functional reconstitution of aquaporin Z proteins

Size distribution of polymersomes was characterized by Nanoparticle Tracking Analyzer (NTA) Nanosight 3.1 Build 3.1.46 (Malvern Panalytical Ltd, UK), equipped with a charge-coupled device (CCD) camera. The camera level was set to 14, slider shutter to 1485, slider gain to 470, and the recording was done with 30 FPS and 3600 number of frames. The samples were diluted 400 times with PBS buffer, resulting in concentrations of 41 (for AQP-0) and 56 (for AQP-1) particles per frame. The measurements were done at 23 °C. Zeta potential of the polymersomes solution has been measured with use of folded capillary cells DTS1070 on a Zeta Sizer Nano (Malvern Panalytical Ltd, UK). The functional reconstitution of AqpZ in polymersomes was analysed with the use of a Stopped-Flow Spectrometer SX20 device (Applied Photophysics Inc, USA), equipped with a 150 W xenon-arc lamp (Osram, Germany), using a monochromator set to a wavelength of 465 nm. For each SF measurement, 10 µL of polymersome solution and 10 µL of 0.5 M NaCl solution were rapidly mixed in a 20 µL optical cell at 25 °C. When polymersomes are exposed to the NaCl solution, the osmotic pressure difference causes water efflux from the polymersomes, resulting in a decrease in volume, thereby causing a change in the refractive index of the solution [38]. The kinetics of these changes are measured by the light scattering detector. The higher the water efflux through the polymersome membrane observed – the more rapid volume change occurs. The kinetics of this process are obtained from the Stopped-Flow Light Scattering (SFLS) measurements by fitting the average of five readings to double exponential equation (1) [19,21,39,40] with use of OriginPro software (OriginLab Corporation, USA):

$$Y = \sum_{i=1}^{N} c_i e^{-k_i t} \tag{1}$$

where Y is light scattering intensity, N is the number of exponential terms ($N = 2$), t is time (s), c_i is relative amplitude and k_i are the exponential coefficients (s^{-1}) (i = 1,2).

Faster exponential coefficient k_2 (s^{-1}) is attributed to the water efflux from the polymersomes [21]. The osmotic water permeability through polymersomes is calculated with equation (2) [21,39–41]:

$$P_f = \frac{k_2}{S_A/V_0} V_w \Delta_{osm} \tag{2}$$

where P_f is osmotic water permeability ($\mu m \cdot s^{-1}$), k_2 is the faster exponential coefficient (s^{-1}), S_A is vesicle surface area (μm^2), V_0 is initial vesicle volume (μm^3), V_w is molar volume of water ($0.018\ L \cdot mol^{-1}$), and Δ_{osm} is the osmolarity difference that drives the vesicle volume change ($osmol \cdot L^{-1}$).

2.3. Preparation of membrane TFC AL

MPD (≥99% for synthesis), ε-Caprolactam (≥99% for synthesis) and TMC (≥99% for synthesis) were obtained from Merck KGaA (Germany) and used as received. Isopar™ E was obtained from Brenntag Nordic A/S (Denmark) and filtered through a mechanical filter (approximately 500 μm) prior to use. Anhydrous citric acid was obtained from Citrique Belge (Belgium) and used as received.

A polysulfone (PSF) ultrafiltration membrane was obtained from Aquaporin A/S (Denmark) and used as the support membrane. The support membrane was stored in DI water overnight prior to AL fabrication.

The PA AL layer was synthesized by an *in-situ* IP reaction between MPD monomer in the aqueous phase and TMC monomer in organic solvent. The PES support membrane was cut into 270 × 170 mm pieces and clipped to stainless-steel frames on the edges. This membrane frame was immersed in a solution containing 3 wt% of MPD and 3 wt% of ε-Caprolactam. The solution also contained 3 wt% of AQP-1 or 3 wt% AQP-0 when polymersomes were loaded to the membrane. The immersion in aqueous solution was 30 s. The excess solution was removed from the surface of the membrane by air gun. Subsequently 50 mL of 0.09 wt% TMC organic solution (in Isopar™ E) was applied to the surface of the horizontally placed membrane frame. After 30 s, the excess of organic solution was poured out and the surface of the membrane was dried with an air gun. The membrane was then immersed for 4 min in the 20 wt% citric acid bath preheated to 70 °C to remove the unreacted amine monomers [42]. Afterwards, the membrane was immersed in the DI water at 70 °C for 2 min. Finally, the membranes were flushed with DI water, removed from the stainless-steel frames and stored in the DI water overnight prior to testing.

2.4. Membrane characterization

2.4.1. Scanning electron microscopy

Cross-sections and surface micrographs of the polyamide layer were taken using a field emission scanning electron microscope (JSM-7610F, JEOL, Japan). All samples were sputter coated (Quorum Q150T ES, United Kingdom) with a 5 nm thick layer of chromium. Cross sections were prepared by breaking the membrane samples in liquid nitrogen with a razor blade. All samples were vacuum dried prior to sputter coating and images were taken at an accelerating voltage of 1.0 kV.

2.4.2. X-ray photoelectron spectroscopy

The X-ray photoelectron spectroscopy (XPS) measurements were done with use of Scanning XPS microprobe Quantera SXM (Physical Electronics, USA). The base pressure was $< 6.6 \times 10^{-8}$ Pa, the power of monochromatic Al Kα ($h\nu = 1486.6$ eV) was 25 W and the current was 2.6 mA. The used beam size was 100 μm. A lower energy electron flood gun was used to supply the missing photoelectrons and Auger electrons. Low energy argon ions were used to remove the surplus of electrons from the electron flood gun. Reference elements were used to calibrate the energy scale.

2.4.3. Zeta (ζ) potential measurements

Zeta potential of the flat sheet membranes was measured using streaming potential measurements with an electrokinetic analyzer (SurPass, Anton Paar, Graz Austria). Two samples were affixed to 10 × 20 mm sample holders with double-sided tape using an adjustable gap cell. Inside the adjustable gap cell a rectangular silicone block ensures the chamber is sealed. The two sample holders were placed opposite each other in the adjustable gap cell creating a rectangular slit between the two membrane samples. The slit, or gap height, was adjusted to 110 μm. A 5 mM KCl solution was allowed to flow through the adjustable gap cell under ambient conditions. Under a given pressure difference, the flow through the cell creates a streaming current. With the measured streaming current (A), dI, and the applied pressure difference (Pa) dp, the zeta potential (V) ζ, can be calculated according to equation (3):

$$\zeta = \frac{\mathrm{dI}}{\mathrm{dp}} \cdot \frac{\eta}{\varepsilon \cdot \varepsilon_0} \cdot \frac{L}{A} \tag{3}$$

where, η is the dynamic viscosity (Pa·s) of the electrolyte, ε the dielectric constant of the electrolyte, ε_0 the permittivity of vacuum ($F \cdot m^{-1}$), L is the length (m) of the streaming channel, and A is the cross-section area (m^2) of the streaming channel. Every membrane sample was measured a minimum of six times in the 5 mM KCl solution and for every measurement point three membrane samples were measured. From this data a standard deviation was derived.

2.5. Membrane performance evaluation

The performance of the prepared TFC membranes was evaluated with a reverse osmosis testing setup containing six CF042P Sterlitech cross-flow cells (Sterlitech Corp., USA). Each sample of the prepared membrane was cut into 3 coupons of 58 mm × 112 mm to fit the CF042P Sterlitech cells. The solution of 500 ppm NaCl (Akzo Nobel Salt A/S, Denmark) was used as a feed and has been circulated through the cells on the side facing the AL of the membrane. The testing pressure applied was 5 bar. The feed solution at 25 °C was introduced into the filtration cell with a flow-rate of 60 Lh^{-1}, which corresponds to the cross-flow velocity of 20 cm/s. Before permeate sample collection, membrane samples were compressed for 30 min. Permeate samples were collected and weighted to obtain liquid permeability (L_p) according to equation (4):

$$L_p = \frac{\Delta V}{\Delta t \cdot A \cdot (\Delta P - \Delta \pi)} \tag{4}$$

where, L_p is the water permeability of the membrane ($L \cdot m^{-2} \cdot h^{-1} \cdot bar^{-1}$), ΔV is the volume of the collected permeate sample (L), Δt is the sampling time (s), A is the active area of the membrane (m^2), ΔP is the applied pressure (bar), and Δπ is the osmotic pressure of the feed solution (bar).

Conductivity of the obtained samples was measured by Ultrameter II 6PFCE (Myron L® Company, USA) and was applied for calculation of NaCl concentration in feed and permeate samples, which was later used to calculate NaCl rejection according to equation (5):

$$R(\%) = \left(1 - \frac{C_p}{C_f}\right) \times 100\% \tag{5}$$

where, R is the membrane salt rejection, C_p is the concentration of NaCl in the permeate, and C_f is the concentration of the NaCl in the feed solution.

3. Results and discussion

3.1. Functional reconstitution of aquaporin Z into polymersomes

The characteristics of polymersomes are summarized in Table 1.

The measurements obtained by NTA show that AQP-1 and AQP-0 have very comparable mean sizes and size distribution, namely 154 ± 1 nm for AQP-1 and 153 ± 3 nm for AQP-0. In both solutions concentration of polymersomes was comparable as well, $3.26 \times 10^{11} \pm 7.08 \times 10^{9}$ nm for AQP-1 and $4.44 \times 10^{11} \pm 1.24 \times 10^{10}$ nm for AQP-0, respectively. This indicates that the presence of AqpZ in the solution does not affect the self-assembly process, and that the formation of polymersomes does not influence the average size nor the concentration of polymersomes. The ζ-potential of both AQP-1 and AQP-0 was similar, +0.9 mV and +0.4 mV respectively, confirming no difference in surface charge between AQP-1 and AQP-0 polymersomes. Measured ζ-potential suggest that the electrostatic repulsion between polymersomes are negligible. It is suspected that the stability of the

Table 1
Size distribution, ζ-potential, pH and osmotic water permeability of PMOXA-PDMS-PMOXA polymersomes. D10, D50 and D90 are particle size distribution intercepts of 10%, 50% and 90%, ± values indicate standard error.

Type of polymersomes	Mean size (nm)	D10 (nm)	D50 (nm)	D90 (nm)	Conc. of polymersomes (particles·mL^{-1})	ζ-potential (mV)	pH	Osmotic water permeability P_f (μm·s^{-1})
AQP-1	154 ± 1	99 ± 1	126 ± 2	234 ± 3	$3.26 \times 10^{11} \pm 7.08 \times 10^{9}$	+0.9	8.03	143 ± 5
AQP-0	153 ± 3	102 ± 1	134 ± 1	208 ± 8	$4.44 \times 10^{11} \pm 1.24 \times 10^{10}$	+0.4	8.10	109 ± 3

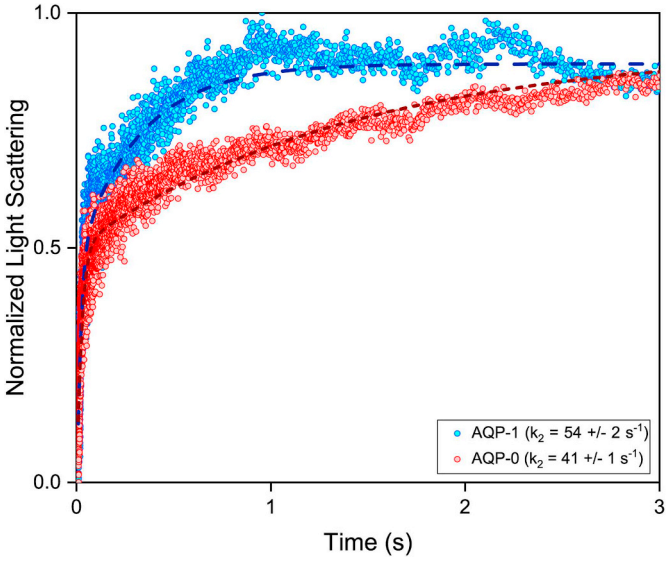

Fig. 1. Stopped-flow light scattering readings for AQP-0 and AQP-1 polymersomes – measured against 0.5 M NaCl at 25 °C. The data points presented here are average values from 5 separate measurements for each sample, while dashed lines represent the fits made with double exponential equation (1).

solution is maintained by steric stabilization induced by the presence of copolymers and surfactants [43]. The faster exponential coefficient obtained from the SFLS experiment (see Fig. 1) was larger for AQP-1 ($k_2 = 54 \pm 2\ s^{-1}$) than for AQP-0 ($k_2 = 41 \pm 1\ s^{-1}$). As a result, osmotic water permeability calculated from the faster exponential coefficient (k_2) was about 32% larger for AQP-1 polymersomes than for AQP-0 polymersomes – 143 ± 5 μm·s^{-1} and 109 ± 3 μm·s^{-1}, respectively (Table 1).

The increased permeability of AQP-1 compared to AQP-0 indicates a successful functional reconstitution of AqpZ into amphiphilic membrane of polymersomes, without influencing other characteristics of polymersomes such as hydrodynamic diameter and zeta potential. In this case, the observed difference in water permeability between AQP-0 and AQP-1 is significantly lower than usually reported in the literature for PMOXA-PDMS-PMOXA polymersomes containing aquaporins.

In multiple articles, authors have reported greater increases in permeabilities of the polymersomes made of PMOXA-PDMS-PMOXA amphiphilic block copolymers. In the early work on AqpZ reconstituting polymersomes, Kumar et al. reported permeabilities of 0.8 μm·s^{-1} for blank polymersomes that increased to 74 μm·s^{-1}, 1500 μm·s^{-1} and 2500 μm·s^{-1} with increased AqpZ loading in the $PMOXA_{15}$-$PDMS_{110}$-$PMOXA_{15}$ measured at 5.5 °C [19]. In a paper from 2012, Zhong et al. reported an increased permeability from 0 μm·s^{-1} for $PMOXA_{10}$-$PDMS_{70}$-$PMOXA_{10}$ blank to 1673 μm·s^{-1}, 2049 μm·s^{-1} and 2350 μm·s^{-1}, however, the temperatures at which the measurements were done are not specified [31]. In another article by Duong and coworkers, no flux is reported for the control disulphide functionalized $PMOXA_{10}$-$PDMS_{75}$-$PMOXA_{20}$ polymersomes, whereas the flux increase to 2595 and 4680 μm·s^{-1} when AqpZ are incorporated (measured at 25 °C) [30]. Grzelakowski et al., using amine functionalized PMOXA-PDMS-PMOXA reports fluxes of 184 μm·s^{-1} for control and 4788 μm·s^{-1} for AqpZ-loaded polymersomes, however, no block lengths are specified, and neither were the temperatures at which the permeabilities were measured [21].

Here, a relatively low increase in permeability of the polymersomes after reconstitution of the AqpZ and high permeability of the blank polymersomes implies that an amphiphilic membrane of prepeared polymersomes is already highly permeable to water. It differs from the previously reported approaches, in which polymersomes show no transport or very limited transport of water through amphiphilic membranes. We speculate that the reason behind increased permeability of blank polymersomes is the effect of the surfactants on the amphiphilic copolymer wall of the vesicles. The surfactant molecules are known to incorporate into the outer leaflet of the polymeric bilayer causing its partial solubilisation [44]. This will cause an enhanced permeability and as the concentration of the surfactant increase, may also lead to disintegration of polymersomes [45]. However, this is not the case in this study, as the size measurement does not imply the presence of a significant population of structures below 100 nm (Table 1).

3.2. Membrane characterization

Biomimetic TFC RO membranes were prepared according to the protocol described in section 2.2. The TFC layer was doped with AQP-0 and AQP-1 polymersomes in order to investigate the effect of aquaporin proteins on the performance and properties of the RO membranes. Membranes without polymerosomes were also prepared as a control of the experiment.

3.2.1. Scanning electron microscopy

SEM micrographs of surface and cross-section of the control membranes, membranes with AQP-0, AQP-1 are presented in Fig. 2.

The addition of polymersomes did not affect the thickness of the polyamide layer. For all membranes, the thickness of the polyamide was comparable - ranging from 200 to 350 nm. However, from the cross-section micrographs it can be seen that the morphology of the control membrane is different than for the AQP-0 and AQP-1 membranes. When polymersomes are introduced, there is a visible increase in the number of hollow spaces within the bulk polyamide layer – both for AQP-0 and AQP-1. The surface morphology of the control membrane was also different when compared to AQP-1 and AQP-0, whereas AQP-1 and AQP-0 are comparable. As polymersomes are expected to take part in the interfacial polymerization reaction through amino-terminated chains of A-PDMS, it is likely that the resulting polyamide layer has a different appearance compared to the membrane without polymersomes. Since AQP-0 and AQP-1 have the same characteristics and the only difference between them is the reconstitution of AqpZ proteins for AQP-1, the same type of TFC layer morphology is observed. The single polymersomes are not visible, as they become an integral part of the polymer matrix when they are covered by it. Due to the size of the AqpZ protein tetramer, which only spans a few nm [46], the morphology difference between AQP-0 and AQP-1 cannot be observed on the SEM micrographs.

3.2.2. X-ray photoelectron spectroscopy

The XPS analysis of the selective layer was made to determine the elemental composition of the formed polyamide film. The concentrations of C, N, O, S and Si in the selective layer, obtained with XPS core

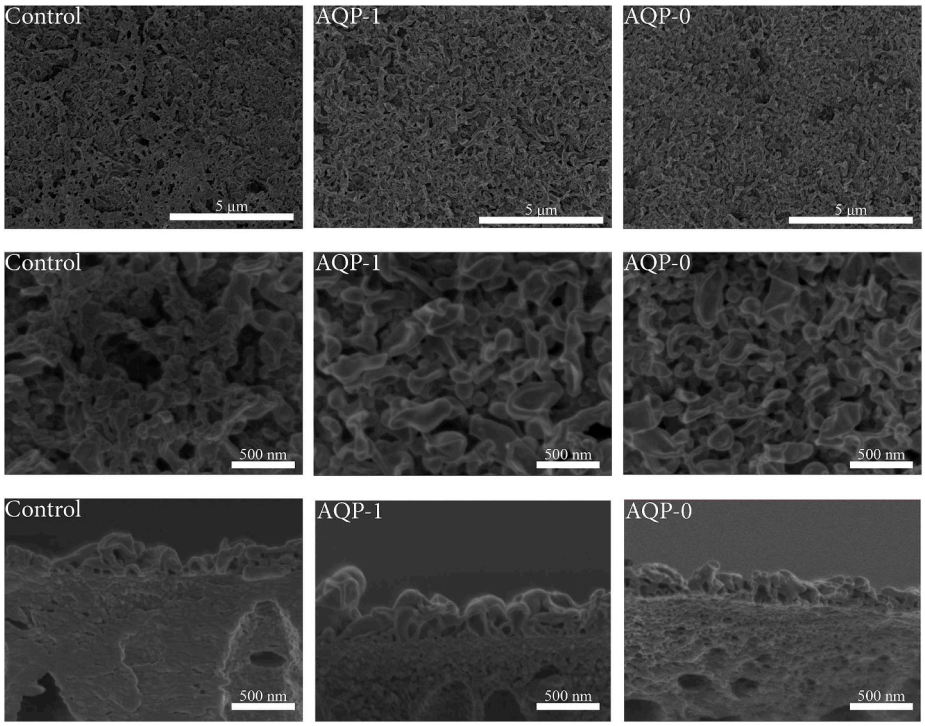

Fig. 2. SEM micrographs of prepared polyamide membranes - Control, AQP-1 and AQP-0. A - top views of the surfaces of polyamide active layer; B - top views of the surface of polyamide active layer; C - cross section of the membranes.

spectra, are listed in Table 2.

In comparison to the support, the concentration of C and O dropped for the control membrane and AQP-0 and AQP-1 membranes, while the concentration of N increased due to the polyamide layer formed on top of the membrane. Regarding the spectra for the polyamide membranes, there is no longer a peak from S, indicating a full coverage of the support with a polyamide thin film for all membrane samples. Concentrations of N decreased by 1.5%, while concentration of O increased by 1–2% for both AQP-0 and AQP-1 membranes in comparison to the control. This indicates that the elemental composition of polyamide formed when polymersomes are introduced differs form the polyamide without polymersomes. We speculate that the elevated concentration of oxygen indicates incorporation of PMOXA-PDMS-PMOXA and amino-PDMS via reaction with TMC. Counterintuitively, the content of Si is the highest for the control membrane and drops for AQP-0 and AQP-1, where Si-containing polymers have been introduced. However, the content of Si is at the lower limit of detection, with a high standard deviation, which may be a result of sample cross contamination, as all of the samples were stored together overnight prior testing.

3.2.3. ζ-potential measurements

The ζ-potential measurements of polyamide membranes and support are presented in Table 3.

As expected, measured ζ-potential for all of the polyamide coated membranes was about 9–16 mV more negative than ζ-potential for the support membrane. Lower ζ-potential of polyamide coated membranes indicated a more negatively charged surface of the membrane and in fact again confirms the successful coating of the polyamide layer on top of the membrane support. The polyamide coated membranes had similar ζ-potential, but for the AQP-0 and AQP-1 doped membranes, the ζ-potential was 5.57–7.12 mV more negative than for the control membrane. Taking into account the accuracy of the measurement method and standard deviations, we assume that this slight change has a minor impact on the separation properties between control membrane and membranes doped with polymersomes: AQP-0 and AQP-1.

Table 3
ζ-Potential of the support, control, AQP-0 and AQP-1 membranes measured at pH 5.5.

Sample name	ζ-potential (mV)	Standard Deviation
Support Membrane	- 20.13	± 1.63
Control Membrane	- 28.93	± 0.34
AQP-0 membrane	- 36.05	± 1.97
AQP-1 membrane	- 34.50	± 0 .77

3.3. Membrane performance

Water permeability and NaCl rejection of the control membranes, membranes doped with AQP-0 and membranes doped with AQP-1 polymersomes are presented in Fig. 3. For each type of RO membrane, 9 coupons were tested.

Table 2
X-ray photoelectron spectroscopy spectra results. Concentrations of C, N, O, S and Si of the support membrane, control membrane, and membranes loaded with AQP-0 and AQP-1.

Sample name	C concentration (%)	N concentration (%)	O concentration (%)	S concentration (%)	Si concentration (%)
Support membrane	77.6 ± 0.6	2.1 ± 0.2	18.1 ± 0.5	2.2 ± 0.1	–
Control membrane	74.3 ± 0.7	11.4 ± 0.3	14.0 ± 0.5	–	0.3 ± 0.1
AQP-0 membrane	74.6 ± 0.7	10.1 ± 0.3	15.2 ± 0.6	–	0.1 ± 0.1
AQP-1 membrane	73.7 ± 0.7	10.1 ± 0.3	16.2 ± 0.8	–	0.1 ± 0.1

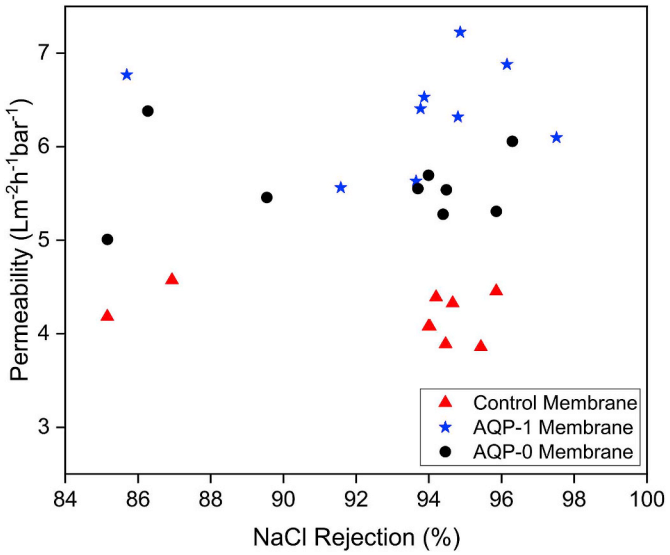

Fig. 3. Water permeability and NaCl rejection of membrane samples without polymersomes, with AQP-0 polymersomes and AQP-1 polymersomes. The membranes were tested at 5 bars with 500 ppm NaCl as feed solution, at 25 °C and feed flow rate of 60 Lh^{-1}.

The control membranes, which are composed of a polyamide layer without polymersomes, resulted in an average water permeability of 4.20 ± 0.25 $L{\cdot}m^{-2}{\cdot}h^{-1}{\cdot}bar^{-1}$ and a NaCl rejection of 92.7 ± 3.9%. The membranes with AQP-0 polymersomes exhibited increased water permeability in comparison to the control membrane: 5.59 ± 0.42 $L{\cdot}m^{-2}{\cdot}h^{-1}{\cdot}bar^{-1}$, while maintaining comparable rejection of NaCl: 92.2 ± 4.1%. The highest average water permeability was observed for the samples prepared with AQP-1, which was 6.38 ± 0.55 $L{\cdot}m^{-2}{\cdot}h^{-1}{\cdot}bar^{-1}$ and NaCl rejection was also maintained at 93.5 ± 3.4%. Statistical analysis with One-Way ANOVA and the Tukey Test was made for each pair of membrane permeability datasets and confirmed that each set of prepared membranes is significantly different from the others (for all comparisons of the pairs, the p-value was always < 0.05, with an overall ANOVA p-value of $4.34 \cdot 10^{-10}$ and an F-value of 60.33 with F-critical of 3.43) (Fig. 4).

Compared to the membranes without polymersomes (control), addition of AQP-0 polymersomes increased water permeability by 33%, while the NaCl rejection was maintained at the same level. Membranes prepared with AQP-1 polymersomes resulted in a further increase in performance, compared to the control, with an improved water permeability of 51% and comparable NaCl rejection. The permeability increase with AQP-1 compared to AQP-0 was 14%. The increased water permeability after addition of AQP-0, clearly indicates that the polymersomes contribute to facilitation of water transport through the TFC active layer, due to high water permeability through their triblock copolymer membrane wall, confirmed by the SFLS. Similarly, Qi et al. used PMOXA-PDMS-PMOXA polymersomes to improve water permeability [39]. Additionally, the improved water permeability can be explained by the incorporation of the hollow nanostructures in the polyamide layer, corresponding to the case recently reported by Ma et al.; in their work, the nanobubbles formed during IP reactions were responsible for the facilitation of water permeability [47]. Here, the AQP-0 polymersomes may play a similar role. Furthermore, NH_2 groups from amino-modified PDMS chains within polymersomes, may compete with MPD in interfacial polymerization reactions. The resulting membrane will be less densely cross-linked, as long PDMS chains will be introduced in the polyamide – the results obtained from XPS clearly indicate that the structure of the formed polyamide has changed (Table 2).

Finally, the use of AQP-1 can increase the water permeability even further than AQP-0. This indicates that AqpZ activity is maintained when AQP-1 are incorporated into the active layer matrix of the membrane. The additional increase in water permeability suggests that the water transport is facilitated through the AqpZ channels, which have been functionally reconstituted to the ABA copolymer membrane of the polymersomes. We speculate that the addition of the amino-modified PDMS during reconstitution of the AQP-0 and AQP-1 polymersomes and the incorporation of those polymer chains into the vesicles allowed for covalent bonding of the polymersomes to the polyamide matrix. As a result, rejection of the NaCl was maintained at the same level for all the tested membranes, even though water permeability increased significantly.

4. Conclusions

Highly permeable NH_2-functionalized triblock PMOXA-PDMS-PMOXA copolymer polymersomes prepared by a bulk hydration method can functionally reconstitute AqpZ proteins. In this study, it has been shown that such polymersomes, which can reconstitute AqpZ water channel proteins can be successfully used for improving the permeability of reverse osmosis membranes without affecting the thickness nor the surface charge of the resulting polyamide layer. Changed elemental composition of the polyamide layer proves that the triblock copolymer is being incorporated into the polyamide. Additionally, incorporation of the blank polymersomes improves water permeability, but an even greater increase in permeability can be achieved with the introduction of Aquaporin Z proteins. The approach for biomimetic membrane fabrication used in this study is based on industrially well-known interfacial polymerization synthesis of polyamide and is therefore relatively easy to upscale to full-size membrane production. Furthermore, since the bulk hydration self-assembly method for preparation of polymersomes does not require multiple steps (such as film rehydration), upscaling of the polymersome production process is also possible. The proposed approach offers great promise for water treatment technology due to the combination of

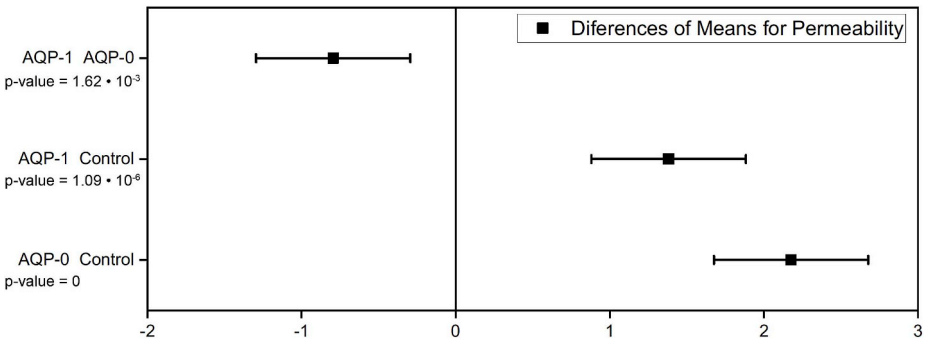

Fig. 4. Tukey test means comparison plot for permeability of different membrane sets. If an interval does not contain 0, the corresponding means of pairs are significantly different.

improved membrane performance coupled with process scalability for large-scale industrial biomimetic membrane manufacturing.

Acknowledgements

The authors would like to thank Dr. Jörg Vogel for support and feedback during the research work and writing this article, Scott Treven Myers for scientific feedback and proof reading and Katrine Veis for language related feedback.

This work is co-founded by Aquaporin A/S and the Innovation Fund Denmark under the project *Development of Next Generation of Aquaporin Inside™ membranes* and EU Horizon 2020 project *Aquaporin-Inside™ Membranes for Brackish water Reverse Osmosis Application (AMBROSIA), grant agreement ID* 783848.

References

[1] B.F. Milan, Clean water and sanitation for all: interactions with other sustainable development goals, Sustain. Water Resour. Manag. 3 (2017) 479–489, https://doi.org/10.1007/s40899-017-0117-4.
[2] United Nations Environment, UN-WATER, The United Nations World Water Development Report 2018: Nature-Based Solutions For Water, UNESCO, Paris, France, 2018www.unesco.org/open-access/.
[3] H.T. Madsen, N. Bajraktari, C. Hélix-Nielsen, B. Van der Bruggen, E.G. Søgaard, Use of biomimetic forward osmosis membrane for trace organics removal, J. Membr. Sci. 476 (2015) 469–474, https://doi.org/10.1016/j.memsci.2014.11.055.
[4] M. Shannon, P.W. Bohn, M. Elimelech, J.G. Georgiadis, B.J. Mariñas, A.M. Mayes, Science and technology for water purification in the coming decades, Nature 452 (2008) 301–310, https://doi.org/10.1038/nature06599.
[5] T. Hey, N. Bajraktari, J. Vogel, C. Hélix Nielsen, J. la Cour Jansen, K. Jönsson, The effects of physicochemical wastewater treatment operations on forward osmosis, Environ. Technol. 0 (2016) 1–13, https://doi.org/10.1080/09593330.2016.1246616.
[6] H.B. Park, J. Kamcev, L.M. Robeson, M. Elimelech, B.D. Freeman, Maximizing the right stuff: the trade-off between membrane permeability and selectivity, Science 356 (2017), https://doi.org/10.1126/science.aab0530.
[7] M.M. Pendergast, E.M.V. Hoek, A review of water treatment membrane nanotechnologies, Energy Environ. Sci. 4 (2011) 1946–1971, https://doi.org/10.1039/c0ee00541j.
[8] H.L. Wang, T.S. Chung, Y.W. Tong, K. Jeyaseelan, A. Armugam, H.H.P. Duong, F. Fu, H. Seah, J. Yang, M. Hong, Mechanically robust and highly permeable Aquaporin Z biomimetic membranes, J. Membr. Sci. 434 (2013) 130–136, https://doi.org/10.1016/j.memsci.2013.01.031.
[9] H. Elfil, A. Hamed, A. Hannachi, Technical evaluation of a small-scale reverse osmosis desalination unit for domestic water, Desalination 203 (2007) 319–326, https://doi.org/10.1016/j.desal.2006.03.530.
[10] D. Li, Y. Yan, H. Wang, Recent advances in polymer and polymer composite membranes for reverse and forward osmosis processes, Prog. Polym. Sci. 61 (2016) 104–155, https://doi.org/10.1016/j.progpolymsci.2016.03.003.
[11] C.Y. Tang, Y. Zhao, R. Wang, C. Hélix-Nielsen, A.G. Fane, Desalination by biomimetic aquaporin membranes: review of status and prospects, Desalination 308 (2013) 34–40, https://doi.org/10.1016/j.desal.2012.07.007.
[12] C. Tang, Z. Wang, I. Petrinic, A.G. Fane, C. Hélix-Nielsen, Biomimetic aquaporin membranes coming of age, Desalination 368 (2014) 89–105, https://doi.org/10.1016/j.desal.2015.04.026.
[13] X. Li, S. Chou, R. Wang, L. Shi, W. Fang, G. Chaitra, C.Y. Tang, J. Torres, X. Hu, A.G. Fane, Nature gives the best solution for desalination: aquaporin-based hollow fiber composite membrane with superior performance, J. Membr. Sci. 494 (2015) 68–77, https://doi.org/10.1016/j.memsci.2015.07.040.
[14] P.A. Pedersen, F.B. Bjørkskov, S. Alvisse, C. Hélix-Nielsen, From channel proteins to industrial biomimetic membrane technology, Faraday Discuss 209 (2018) 287–301, https://doi.org/10.1039/c8fd00061a.
[15] C. Helix-Nielsen, Biomimetic Membranes for Sensor and Separation Applications, (2015), https://doi.org/10.1017/CBO9781107415324.004.
[16] C.G. Palivan, R. Goers, A. Najer, X. Zhang, A. Car, W. Meier, Bioinspired polymer vesicles and membranes for biological and medical applications, Chem. Soc. Rev. 45 (2016) 377–411, https://doi.org/10.1039/C5CS00569H.
[17] M.P. Grzelakowski, Novel Polymers and Process for Making Membranes, (2015) WO 2015/144725 A1.
[18] F. Itel, A. Najer, C.G. Palivan, W. Meier, Dynamics of Membrane Proteins within Synthetic Polymer Membranes with Large Hydrophobic Mismatch, (2015), https://doi.org/10.1021/acs.nanolett.5b00699.
[19] M. Kumar, M. Grzelakowski, J. Zilles, M. Clark, W. Meier, Highly permeable polymeric membranes based on the incorporation of the functional water channel protein aquaporin Z, Proc. Natl. Acad. Sci. U.S.A. 104 (2007), https://doi.org/10.1073/pnas.0708762104 20719–24.
[20] H. Wang, T.S. Chung, Y.W. Tong, K. Jeyaseelan, A. Armugam, Z. Chen, M. Hong, W. Meier, Highly permeable and selective pore-spanning biomimetic membrane embedded with aquaporin Z, Small 8 (2012) 1185–1190, https://doi.org/10.1002/smll.201102120.
[21] M. Grzelakowski, M.F. Cherenet, Y. xiao Shen, M. Kumar, A framework for accurate evaluation of the promise of aquaporin based biomimetic membranes, J. Membr. Sci. 479 (2015) 223–231, https://doi.org/10.1016/j.memsci.2015.01.023.
[22] M.P. Grzelakowski, Novel Polymers and Process for Making Membranes, (2018) WO 2015/144725.
[23] D. Wu, M. Spulber, F. Itel, M. Chami, T. Pfohl, C.G. Palivan, W. Meier, Effect of molecular parameters on the architecture and membrane properties of 3D assemblies of amphiphilic copolymers, Macromolecules 47 (2014) 5060–5069, https://doi.org/10.1021/ma500511r.
[24] N. Muhammad, T. Dworeck, M. Fioroni, U. Schwaneberg, Engineering of the E . Coli outer membrane protein FhuA to overcome the hydrophobic mismatch in thick polymeric membranes, J. Nanobiotechnol. 9 (8) (2011) 1–9.
[25] M. Spulber, D. Tvermoes, R. Górecki, F. Haugsted, Vesicle Incorporating Transmembrane Protein, (2019) WO 2019/081371 A1.
[26] Y. Zhao, C. Qiu, X. Li, A. Vararattanavech, W. Shen, J. Torres, C. Hélix-Nielsen, R. Wang, X. Hu, A.G. Fane, C.Y. Tang, Synthesis of robust and high-performance aquaporin-based biomimetic membranes by interfacial polymerization-membrane preparation and RO performance characterization, J. Membr. Sci. 423–424 (2012) 422–428, https://doi.org/10.1016/j.memsci.2012.08.039.
[27] R. Sengur-Tasdemir, B. Sayinli, G.M. Urper, H.E. Tutuncu, N. Gul-Karaguler, E. Ates-Genceli, V.V. Tarabara, I. Koyuncu, Hollow fiber nanofiltration membranes with integrated aquaporin Z, New J. Chem. 42 (2018) 17769–17778, https://doi.org/10.1039/C8NJ04367A.
[28] X. Li, C.H. Loh, R. Wang, W. Widjajanti, J. Torres, Fabrication of a robust high-performance FO membrane by optimizing substrate structure and incorporating aquaporin into selective layer, J. Membr. Sci. 525 (2016) 257–268, https://doi.org/10.1016/j.memsci.2016.10.051.
[29] D.E. Discher, A. Eisenberg, Polymer vesicles, Science 297 (2002) 967–973.
[30] P.H.H. Duong, T.S. Chung, K. Jeyaseelan, A. Armugam, Z. Chen, J. Yang, M. Hong, Planar biomimetic aquaporin-incorporated triblock copolymer membranes on porous alumina supports for nanofiltration, J. Membr. Sci. 409–410 (2012) 34–43, https://doi.org/10.1016/j.memsci.2012.03.004.
[31] P.S. Zhong, T.S. Chung, K. Jeyaseelan, A. Armugam, Aquaporin-embedded biomimetic membranes for nanofiltration, J. Membr. Sci. 407–408 (2012) 27–33, https://doi.org/10.1016/j.memsci.2012.03.033.
[32] L. Xia, M.F. Andersen, C.H. Nielsen, J.R. McCutcheon, Novel commercial aquaporin flat-sheet membrane for forward osmosis, Ind. Eng. Chem. Res. (2017) 11919–11925, https://doi.org/10.1021/acs.iecr.7b02368.
[33] W. Xie, F. He, B. Wang, T.-S. Chung, K. Jeyaseelan, A. Armugam, Y.W. Tong, An aquaporin-based vesicle-embedded polymeric membrane for low energy water filtration, J. Mater. Chem. A. 1 (2013) 7592, https://doi.org/10.1039/c3ta10731k.
[34] D. Li, Y. Yan, H. Wang, Recent advances in polymer and polymer composite membranes for reverse and forward osmosis processes, Prog. Polym. Sci. (2016), https://doi.org/10.1016/j.progpolymsci.2016.03.003.
[35] A. Wagner, K. Vorauer-Uhl, Liposome technology for industrial purposes, J. Drug Deliv. 2011 (2011) 1–9, https://doi.org/10.1155/2011/591325.
[36] X. Sui, P. Kujala, G.J. Janssen, E. De Jong, I.S. Zuhorn, J.C.M. Van Hest, Robust formation of biodegradable polymersomes by direct hydration, Polym. Chem. 6 (2015) 691–696, https://doi.org/10.1039/c4py01288g.
[37] M. Spulber, K. Gerstandt, Diblock Copolymer Vesicles and Separation Membranes Comprising Aquaporin Water Channels and Methods of Making and Using Them, (2018) WO 2018/141985 A1.
[38] A. Horner, P. Pohl, Single-file transport of water through membrane channels, Faraday Discuss 209 (2018) 9–33, https://doi.org/10.1039/c8fd00122g.
[39] S. Qi, W. Fang, W. Siti, W. Widjajanti, X. Hu, R. Wang, Polymersomes-based high-performance reverse osmosis membrane for desalination, J. Membr. Sci. 555 (2018) 177–184, https://doi.org/10.1016/j.memsci.2018.03.052.
[40] F.B. Bjørkskov, S.L. Krabbe, C.N. Nurup, J.W. Missel, M. Spulber, J. Bomholt, K. Molbaek, C. Helix-Nielsen, K. Gotfryd, P. Gourdon, P.A. Pedersen, Purification and functional comparison of nine human Aquaporins produced in Saccharomyces cerevisiae for the purpose of biophysical characterization, Sci. Rep. 7 (2017), https://doi.org/10.1038/s41598-017-17095-6.
[41] H.X. Gan, H. Zhou, Q. Lin, Y.W. Tong, Quantification of Aquaporin-Z reconstituted into vesicles for biomimetic membrane fabrication, Sci. Rep. 7 (2017) 1–13, https://doi.org/10.1038/s41598-017-11723-x.
[42] M. Chau, H. Chu, W. Light, Dry High Flux Semipermeable Membranes, (1991) WO 91/08828.
[43] T. Tadros, Colloid and Interface Aspects of Pharmaceutical Science, Elsevier B.V., 2014, https://doi.org/10.1016/B978-0-444-62614-1.00002-8.
[44] V. Pata, F. Ahmed, D.E. Discher, N. Dan, Membrane solubilization by Detergent : resistance conferred by thickness, Langmuir 20 (2004) 3888–3893, https://doi.org/10.1021/la035734e.
[45] S. Pispas, Vesicular structures in mixed block copolymer/surfactant solutions, Soft Matter 7 (2011) 8697–8701, https://doi.org/10.1039/c1sm05584d.
[46] A.S. Verkman, A.K. Mitra, Structure and function of aquaporin water channels, Am. J. Physiol. Renal. Physiol. 278 (2000) F13–F28, https://doi.org/10.1002/mus.20766.
[47] X.H. Ma, Z. Yao, Z. Yang, H. Guo, Z. Xu, C.Y. Tang, M. Elimelech, Nanofoaming of polyamide desalination membranes to tune permeability and selectivity, Environ. Sci. Technol. Lett. 5 (2018) 123–130, https://doi.org/10.1021/acs.estlett.8b00016.